Convolutional Neural Network for POC Microscopy Image Diagnosis

C.Kalimuthu
Department of CEN, ASE
Amrita University

Work derived from Quinn et al., 2016

Introduction

One of the key medical diagnostics in the medical field is microscopy method. It is used to diagnose many different medical conditions and diseases such as Malaria, tuberculosis etc. Though there are other methods like flow cytometry or molecular biology, they are expensive compared to the microscopy method. The microscopy method compared to be cheaper of them all.

But the microscopy method needs skilled technician for proper diagnosis. According to a study in Ghana, the availability seems that only 1.72 microscopes per 0.1 million people and 0.85 trained lab staff per 0.1 million people (Bates et al., 2004). When there is an epidemic burst, it is obvious that the resources are not enough and most of the diagnosis shall be made based on the expressive signs and symptoms and it has a negative side of higher mortality, drug resistance and economic burden because of the unnecessary usage of the medicines.

So, it is nice to have a new method which does not exist, cheaper and as accurate as possible. A new method with a microscope and a mobile phone is discussed, experimented and documented (Quinn et al.,2016). This document reviews the such implementation and its results.
As discussed in this publication, the focus is on using the deep learning methods for microscopy based PoC diagnostics in a resource constrained environment. One advantage of the deep learning method is that the features need not be handcrafted

Objective:

Deploy a computer vision method for decision support and automated point of care diagnostics

Methodology:

Convolution neural network, being the top method for image recognition, is used

The most commonly available mobile phones with camera are used for capturing the image of the blood, sputum or faeces samples.

Standard microscope deployment is avoided either because of their inter dependency in their mechanical setup and imaging solutions or its cost. So, attachment mechanism which couples the mobile phone with the microscope is 3d printed as shown in the figure 1.

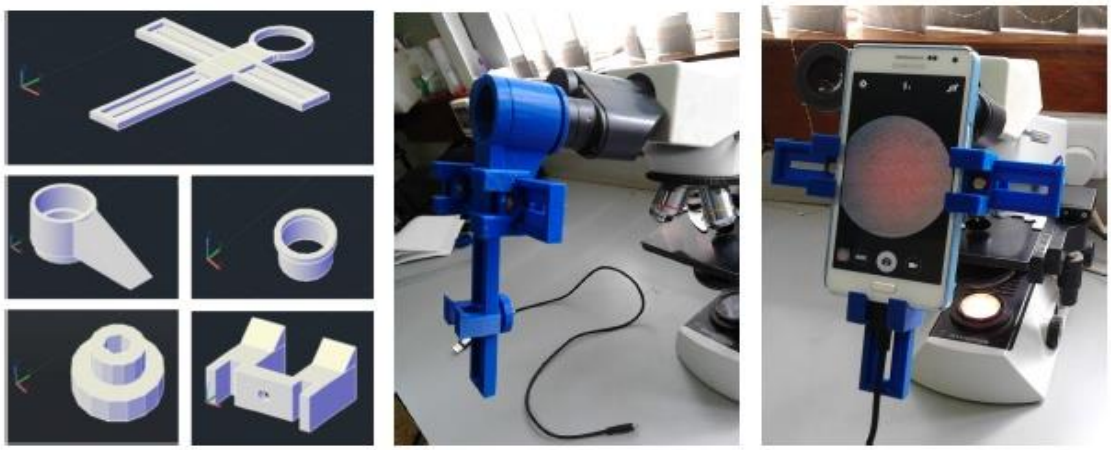

Figure 1: Microscope smartphone adapter: design of components (left), 3D-printed adapter mounted on microscope (center), smartphone inserted into adapter (right).

Images hand marked by the skilled technicians are used as the training and testing samples. Image recognition accuracy is compared with the testing samples once training is done with the training samples.

CNN Architecture

The Convolutional neural network is known for its efficiency in image processing. In conventional densely connected MLP (Multi Layer Perceptron) for image processing, the number of learnable parameters is very high. In CNN, the image is divided into small receptive fields and the weights are shared among them so that the number learnable parameters limited to that convolution filter size. There may be so many filters which respond to the different types of features of the image. In the bottom layers, these responses may be edges, blobs or colours etc and in the higher layers of CNN responds to the more complex patterns. CNN architecture may contain the below layers normally

1. Convolution layer - Convolution layers are computed by taking a sliding window (the receptive field) across the input, calculating the response function at each location for each filter. Multiple filters capture different types of patterns
2. Pooling Layer - Pooling layers reduce the size of the input, merging neighbouring elements e.g by taking the maximum. This reduces the number of parameters, and hence the amount of computation, as each pooling is done.
3. Fully connected layer - Fully connected layers have connections from all activations in the previous layer to all outputs. This is equivalent to a convolutional layer with one filter, the same size. A fully connected layer is typically used as the last layer in a CNN, with
   the output having one element per class label

A typical configuration with 4 hidden layers along with one input and output layer is shown in picture 2. The hyperparameters of the architecture is given as below including input layer and the output layer. All the neurons use RELU activation function except the output layer which uses the softmax

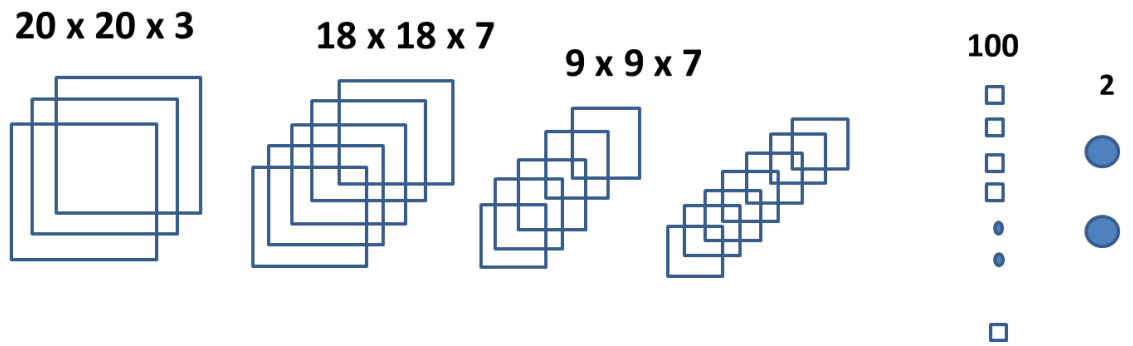

Figure 2: Typical CNN Architecture

Other important hyper parameters are,
The input images are clipped as 20X20 and 60X60 images with depth 3 for RGB colour
The total images are split 50:50 for training and testing.
The training was done for 10,500,500 epochs on each of the three data sets (malaria, Tuberculosis and intestinal parasites) respectively
Given the above architecture, the learnable parameters are restricted to different disease are as below:

Plasmodium(malaria) - Neural Network with 386046 learnable parameters

Layer information

#	name	size
0	input	3x20x20
1	conv1	7x18x18
2	pool1	7x9x9
3	conv2	12x8x8
4	hidden3	500
5	output	2

Intestinal Parasites - Neural Network with 356234 learnable parameters

Layer information

name size

--- ------ -------

0 input 3x60x60

1 conv1 7x56x56

2 pool1 7x28x28

3 lstm 7x100

4 output 2

Tuberculosis - Neural Network with 27448 learnable parameters

Layer information

name size

--- ------ -------

0 input 3x20x20

1 conv1 7x18x18

2 pool1 7x9x9

3 lstm 7x50

4 output 2

Just by considering the input layer and the 100-neuron last stage fully connected layer, in MLP case, the number of neurons would have been 20*20*3*100 = 120,000. Far above the fully functional convolutional neural network described first earlier. The last two outputs at the softmax layers classifies between objects of interest is available or not. The outputs of respective class (yes or no) will have relatively higher value to mark the presence or absence.

Dataset Description

A microscopy image is bigger in size limited by the resolution of the mobile camera used for capturing the image. There the objects of interest can be in the different locations. A patch size of 20X20 is used for Malaria and Tuberculosis and 60X60 is used for intestinal parasites. All images taken for testing is with positive markers somewhere in the image. The location of the positive markers bound with a bounding box and its co-ordinates are mentioned in a corresponding xml file.

With the use of these xml file, the positive markers are identified and patched for positive samples. The rest of the area in the image was taken for negative samples. The number of positive samples were increased by flipping and rotating the samples. The negative samples count also restricted such that the positive samples will be more than 10%

Sample sizes are given below:

Malaria:

28440 positive training examples, 260855 negative training examples

29520 positive testing examples, 259605 negative testing examples

578420 patches (10.0% positive)

Intestinal Parasite:

576 positive training examples, 909 negative training examples

77 positive testing examples, 853 negative testing examples

2415 patches (27.0% positive)

Tuberculosis:

33504 positive training examples, 44979 negative training examples

35840 positive testing examples, 44445 negative testing examples

158768 patches (43.7% positive)

Results:

The figures below show the Plasmodium (malaria)

Figure 3 shows the manually marked image patches for positive and negative plasmodium

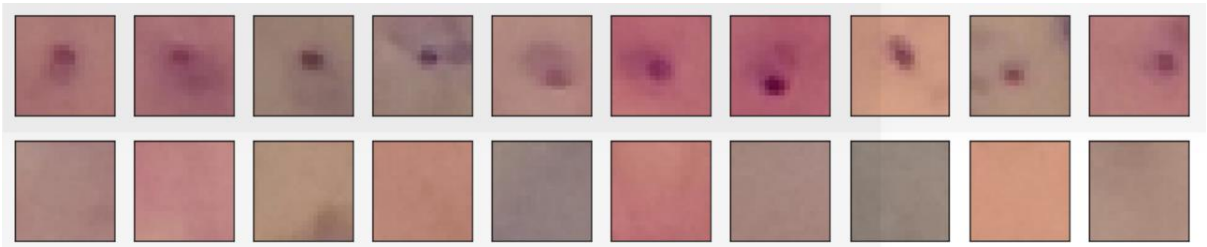

Figure 3: Manually identified. Top – Patches with Plasmodium (Positive), Bottom – Patches without plasmodium (Negative)

Figure 4 shows the CNN identified true positive cases, Figure 5 shows the false positive cases and Figure 6 identifies low probability cases

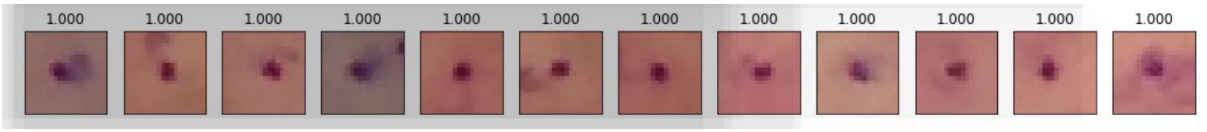

Figure 4: True positive cases by the CNN

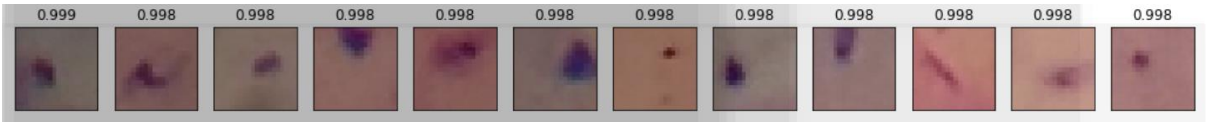

Figure 5: False positive cases detected by the CNN

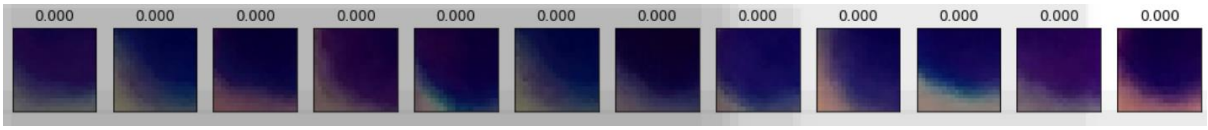

Figure 6: Low probability cases by the CNN

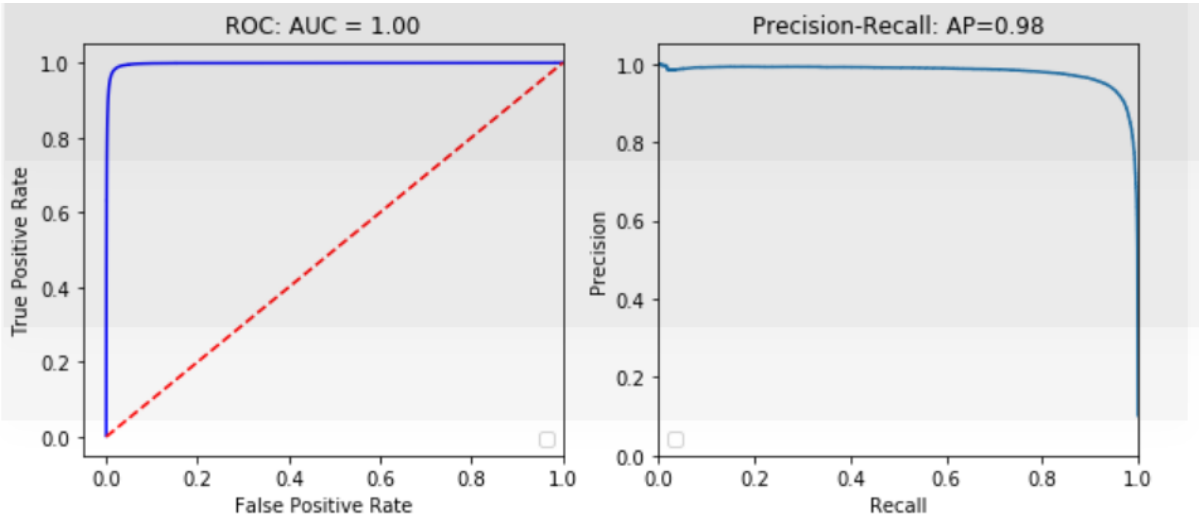

Figure 7: ROC, PR curve for plasmodium detection

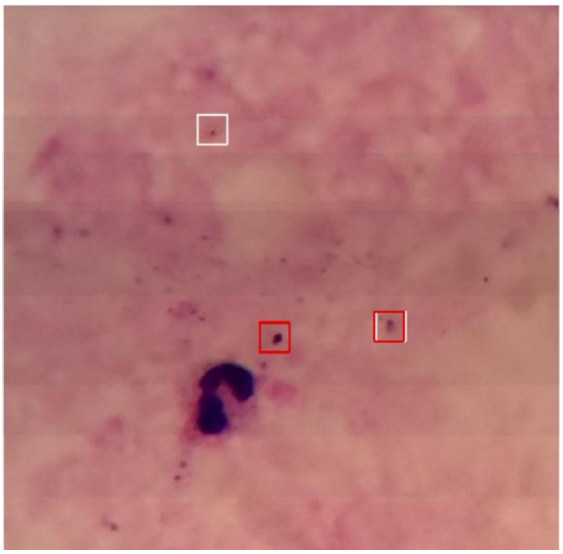

Figure 8: Image with positive markers. White bounding boxes are marked manually. The red bounding boxes are marked by system

Intestinal Parasites:

The figure 9 below shows the hookworm egg presence and absence in the sample

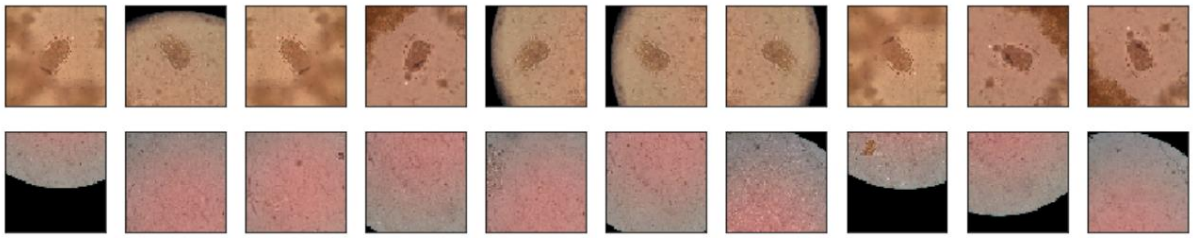

Figure 9: Top – Presence of Hookworm eggs, Bottom – Absence of hookworm eggs

Figure 10 shows the CNN identified true positive cases, Figure 11 shows the false positive cases and Figure 12 identifies low probability cases

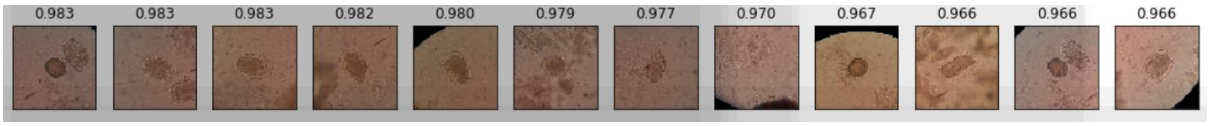

Figure 10 : True positive cases by the CNN

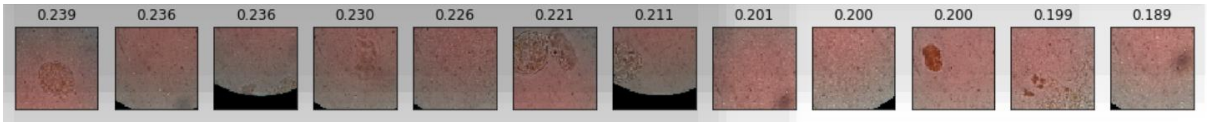

Figure 11: False positive cases by the CNN

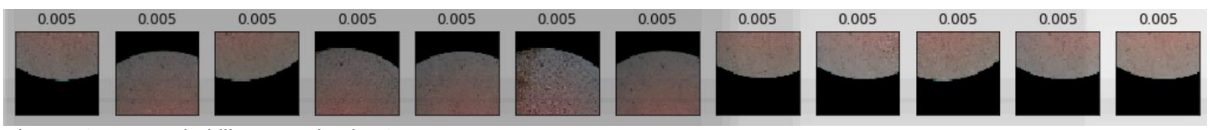

Figure 12: Low probability cases by the CNN

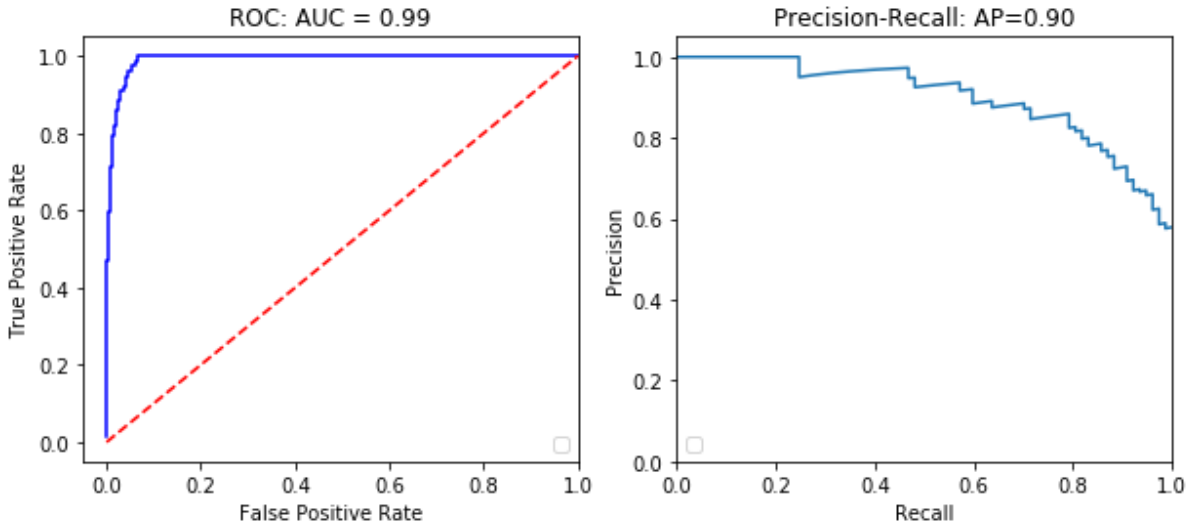

Figure 13: ROC, PR curves intestinal parasites (Hookworm egg) detection

Tuberculosis

Figure 14 below shows the tuberculosis bacilli presence and absence in the sample

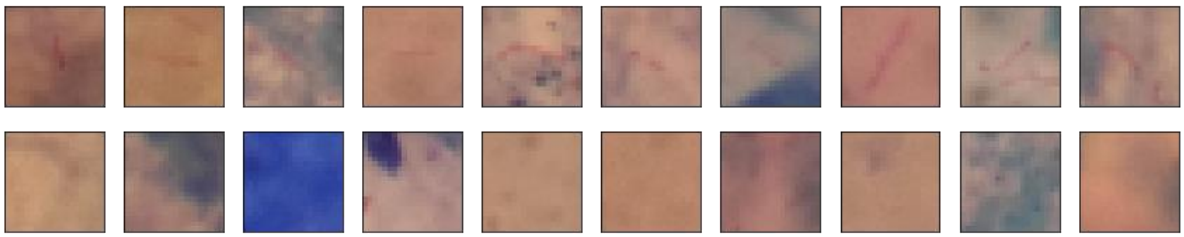

Figure 14: Top – Presence of tuberculosis bacilli, Bottom – absence of tuberculosis bacilli

Figures 15,16 and 17 shows true positive, false positive and low probability cases respectively

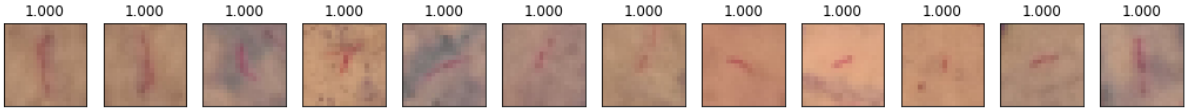

Figure 15: True positive cases

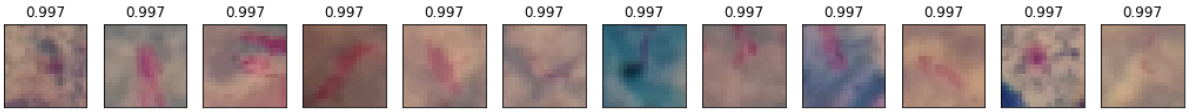

Figure 16: False positive cases

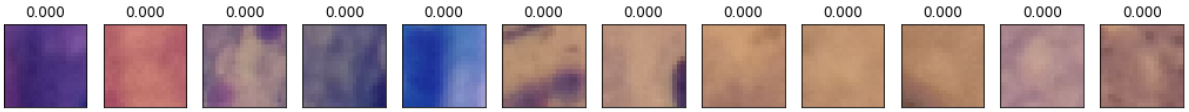

Figure 17: Low probability cases

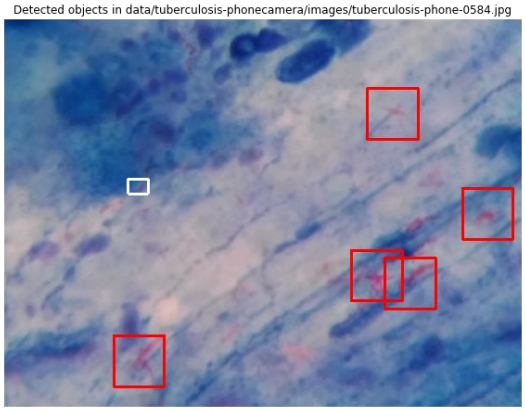

Figure 18: Image with positive markers. White bounding boxes are marked manually. The red bounding boxes are marked by system

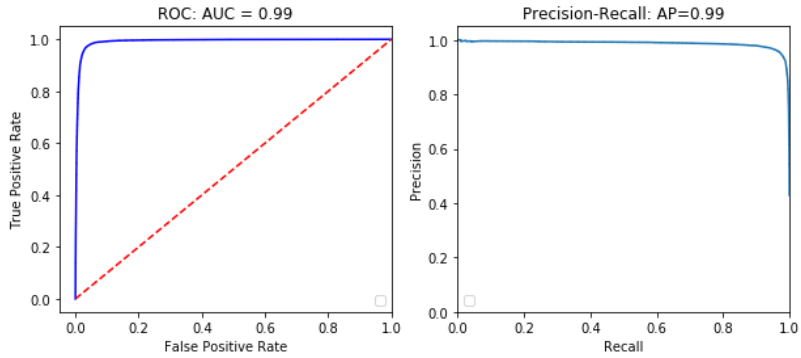

Figure 19: ROC and PR curves (Tuberculosis)

Interpretation

The efficiency of the deep learning method was compared with the traditional method of computer vision where the shape features are extracted and applied to the classifier. The shape features used are a set of morphological and moment statistics as described in the methodology (Quinn et al., 2014) and applied to Extremely randomised tree classifier (Guerts et al., 2006) with 100 trees.

The results are compared using ROC and PR curves as shown in the figures below. The higher the AUC is better.

The Deep learning outperforms the traditional classifier.

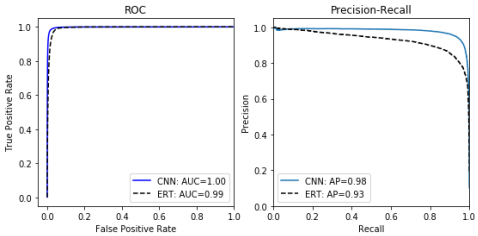

Plasmodium (Malaria)

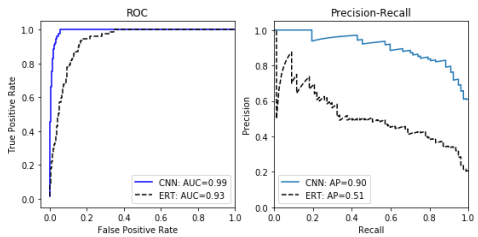

Hookworm egg (Intestinal parasites)

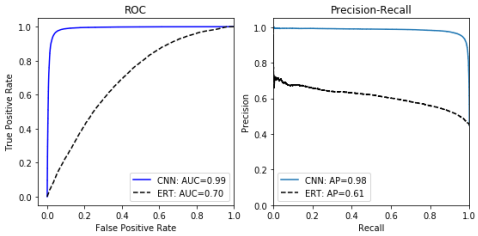

Tuberculosis Bacilli

Conclusion

A point of care diagnostic system for microscopic images were built and tested. The results are satisfactory. So, this system can be used as a decision support tool. This further not demands any expensive microscopy solutions or skilled technicians.

References:

[1] John A. Quinn, Rose Nakasi, Mugagga, Patrick Byanyima, Lubega, Alfred Andama, “Deep Convolutional Neural Networks for Microscopy-Based Point of Care Diagnostics,” in Proceedings of International Conference on Machine Learning for Health Care 2016, JMLR W&C Track Volume 56, 2016

[2] Anson Simon, Vinayakumar R, Dr V Sowmya, Dr K P Soman, “Deep BioMed – 2018,”